Green Chemistry

Accepted Manuscript

ROYAL SOCIETY OF CHEMISTRY

www.rsc.org/greenchem

One-step propylene formation from bio-glycerol over Molybdena-based catalysts

Vasiliki Zacharopoulou[a], Efterpi S. Vasiliadou[a], Angeliki A. Lemonidou [a,b*]

[a] Department of Chemical Engineering, Aristotle University of Thessaloniki, University Campus, Thessaloniki 54124, Greece

[b] Chemical Process Engineering Research Institute (CERTH/CPERI), P.O. Box 60361 Thermi, Thessaloniki 57001, Greece

Corresponding author

Angeliki A. Lemonidou

Phone: +30 2310 996273

Fax: +30 2310 996184

Email: alemonidou@cheng.auth.gr

Abstract

This work presents a novel, one-step catalytic process, enabling highly selective propylene formation via glycerol hydro-deoxygenation (HDO) reaction. Fe-Mo catalysts, supported on black and activated carbons, are selective towards C-O bond cleavage, thus converting glycerol to propylene with high yields. BET, XRD, TPD-NH_3 and TPD-He methods have been employed for the characterization of the samples. Molybdenum oxide, at its reduced state, is essential for driving selectively the reaction towards complete deoxygenation. The only product of glycerol HDO is propene, in the gas phase, while 2-propenol, propanols and propylene glycol have been detected, among others, in the liquid phase. At the standard reaction conditions (300°C temperature, 8.0 MPa hydrogen pressure), glycerol conversion exceeds 88% and selectivity to propene reaches 76%, after 6 hours of reaction. This study includes the investigation of operating conditions effect (*i.e.* reaction time, reaction temperature, catalyst loading and H_2 pressure) regarding glycerol HDO towards propene formation.

1. Introduction

The finite stocks of fossil resources, as well as the rise of environmental issues concerning their increased use, have triggered the exploration and development of alternative feedstocks for the production of transportation fuels and chemical products[1]. Biomass (*e.g.* wood, agricultural crops, algae, as well as their residues and wastes)[2] and biomass-derived compounds (*e.g.* glucose, glycerol, sorbitol, lactic acid) can be effectively used in the production of liquid fuels and platform chemicals[3]- apart from electricity and heat generation, as they are a valuable renewable source of carbon[4]. The above-mentioned feedstocks contain C-O and C-H bonds; therefore, in order for them to be converted into value-added products, the selective cleavage of C-O over C-C bonds is essential. The removal of oxygen from these compounds can be realized through promising hydrogenolysis or hydro-deoxygenation processes[1,4].

Glycerol is one of the twelve top building block chemicals derived from biomass that can be upgraded to high added-value products[5]. It is typically obtained as a by-product of processes such as transesterification of oils and fats, soap manufacture, fatty acid production, fatty ester production, microbial fermentation or enzymatic catalysis, as well as by lignocellulose via catalytic decomposition and through catalytic hydrogenolysis of sorbitol[6-11]. Increased biodiesel production worldwide has led to massive glycerol supply in the market, thus affecting its price. As a result, glycerol is considered a low cost, alternative feedstock that can also be used as a model compound, hence serving as a building block[1]. Glycerol can be converted into various valuable products, i.e. ethylene and propylene glycols[12-16], acetol[17], acrolein[3,18,19], fuel additives[20].

The partial or complete removal of oxygen from the glycerol molecule, via hydro-deoxygenation (HDO) reaction, leads to 1,2- and 1,3-propanediol[12], propanols[21] and propane[22] formation. The latter requires non-active to C-C bond scission catalysts, because during HDO reactions oxygen is removed, in the form of H_2O molecules and not as CO_2. Complete removal of oxygen, along with formation of an unsaturated C=C bond, thus enabling glycerol conversion to propylene, is the desirable, yet challenging, reaction path (Scheme 1). Despite the significant progress in glycerol transformation technologies, glycerol selective conversion to propylene has not yet been thoroughly explored in the open literature. Nevertheless, bio-propylene production has received considerable attention over the past decade[23,24]. Propylene is one of the most important olefins used in the petrochemical industry. It is used as a feedstock for the production of polypropylene, acrylonitrile, propylene oxide, cumene, isopropyl alcohol, acrylic acid and acrolein, among others. Propylene is mainly produced as a co-product of naphtha cracking and as a by-product of fluid catalytic cracking.[25]

Recently, the production of lower hydrocarbons from glycerol has been explored in a patent by Hulteberg and Brandin, describing the catalytic conversion of glycerol to alkanes and alkenes such as ethane, propane and propene, over WO_3 on ZrO_2 and Pt on CeO_2 catalysts[26]. The research of Cao et al. also focuses on the production of propene from glycerol, mainly in a two-step reaction, *i.e.* glycerol hydrogenolysis to 1-propanol, followed by the well-known process of 1-propanol dehydration to produce propene, using Ir/ZrO_2 and HZSM5 catalysts. Moreover, the same group conducted preliminary experiments of direct glycerol conversion to propene with very interesting results, over a combination of the above-mentioned catalysts. [27]

In another patent, Fadigas et al. explored a catalytic process for the production of propene via hydro-deoxygenation of glycerol, over a Fe-Mo/C catalyst, in gas phase[28].

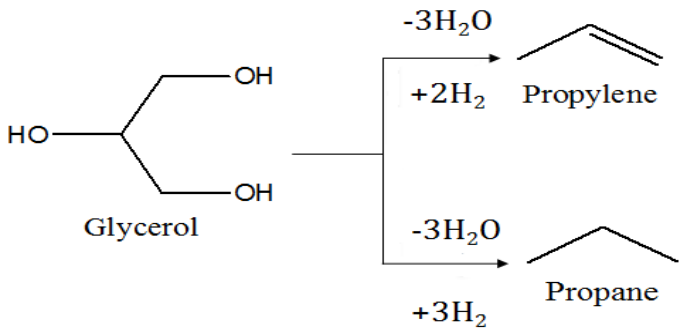

Scheme 1. Glycerol Hydro-deoxygenation Pathways

Triggered by the promising performance of the Fe-Mo/C catalyst described in the above-mentioned patent, this work aims at the investigation of this new route of one-step propylene production, in the liquid phase. The effect of the reaction parameters is of great importance because they possibly affect the yield to the desired product. The present study includes synthesis, detailed characterization and performance evaluation of Fe-Mo catalysts, supported on different carbons (*i.e.* black and activated carbon). More specifically, the effect of reaction parameters, *i.e.* reaction time, reaction temperature, H_2 pressure and catalyst loading, on the reaction performance has been studied. Product distribution with glycerol conversion was used as a guide in order to explore the various reaction routes and principally the propene formation pathway.

2. Experimental section

Support Materials and Precursors

Fe-Mo catalysts were supported on commercially available Black Carbon Vulcan XC72 (Cabot) and on Activated Carbon D10 (Norit). Iron nitrate - $Fe(NO_3)_3 \cdot 9H_2O$ (Fluka) and MoO_3 were used as precursor compounds for Fe and Mo respectively. MoO_3 was synthesized through calcination of the ammonium molybdenum $(NH_4)_6Mo_7O_{24}.4H_2O$ (Fischer) at 500ºC for 2h, under synthetic air flow (100 cm^3 min^{-1}).

Catalyst Synthesis

Fe-Mo catalysts were synthesized by combining wet impregnation and co-precipitation methods, according to the procedure described by Fadigas et al.[27].

The obtained catalysts were calcined at 200ºC, under synthetic air or nitrogen flow (100 cm^3 min^{-1}), for 2h. The specific calcination temperature was selected as carbon supports may burn or smolder at temperatures above 300 ºC. For the same reason catalysts were calcined not only under air flow, but also under inert atmosphere (nitrogen flow). The atomic Mo/Fe ratio of Fe-Mo/C samples is 4:1, while their loading of Fe and Mo (2.7 and 19.3% wt, respectively) was not diverged. Catalysts were pre-reduced, at 500 ºC for 0.5h, under H_2 flow (40 cm^3 min^{-1}).

In order to study the contribution of each metal to the catalytic performance, catalysts containing only Fe or Mo, were also prepared. These samples were dried, calcined and pre-reduced, following the same procedure as with the Fe-Mo catalysts.

All the catalytic samples synthesized in this study are presented in Table 1. BC stands for Carbon Black while AC for Activated Carbon. "A" and "B" signify calcination under air and nitrogen flow, respectively.

Table 1. Synthesized Catalytic Samples

Catalyst	Support	Fe (wt %)	Mo (wt %)	Calcination Atmosphere
Mo/BC_A	Carbon Black	-	20.8	Air
Fe/BC_A	Carbon Black	3.7	-	Air
Fe-Mo/BC_A	Carbon Black	2.7	19.3	Air
Fe-Mo/AC_A	Activated Carbon	2.7	19.3	Air
Fe-Mo/BC_B	Carbon Black	2.7	19.3	N_2
Fe-Mo/AC_B	Activated Carbon	2.7	19.3	N_2

Catalyst Characterization

BET surface areas, pore volumes and average pore diameters were determined by N_2 physisorption at 77K, using an Autosorb-1 Quantachrome flow apparatus. Prior to measurements, samples were dried in vacuum overnight, at 250ºC. The total pore volume was defined as the single point pore volume at a relative pressure of p/p_o=0.95.

XRD patterns of the catalysts were obtained using a D500 diffractometer (Siemens) X-ray with Cu Ka radiation (λ=1.54Å) at a scan rate of 0.02°/sec (2θ) from 5.0º-80.0º.

TGA experiments were carried out on SDT Q600 (TA Instruments) apparatus. SDT Q600 works in conjunction with a controller and associated software to constitute a thermal analysis system. A small amount of the sample was placed in an aluminum

sample cup and then heated from room temperature to 800 ºC at 10 ºC/min, under air or nitrogen flow (100 cm^3 min^{-1}).

Temperature-Programmed Desorption of Ammonia and Temperature-Programmed desorption, in inert (Helium) atmosphere, as well as Temperature-Programmed Reduction and Thermogravimetric Analysis, have also been employed for sample characterization (see SI).

Catalyst Activity Test

Glycerol hydro-deoxygenation experiments were conducted in a 450ml stainless-steel batch reactor (Parr Instruments), equipped with an electronic temperature controller, a heating mantle, a mechanical stirrer, a pressure gage as well as gas inlet and outlet lines. The typical reaction conditions were: 300°C temperature, 8.0 MPa hydrogen pressure, 1.50 g catalyst weight, 90.0 ml of 2.0 w/w % aqueous glycerol solution, 2.0 h reaction time and 800 rpm stirring speed. The experimental procedure consisted of the following steps: feed solution preparation, reactor vessel loading with the catalyst and the feed solution, N_2 flushing for 10 min at 0.2 MPa and leak check at 8.0 MPa for 20 min, H_2 flushing for 5 min at 0.5 MPa, pressurized vessel with 8.0 MPa of H_2, temperature controller set at 300 ºC and then, heater and agitator were turned on. The time at which temperature reaches the set point is considered the zero point, t=0. After 2h of reaction time, heater and agitator were turned off and the vessel was forced to immediately cool to room temperature.

Reaction time effect has been explored up to 6h of reaction. In order to study the effect of temperature, experiments have been conducted at 260, 280 and 300^{o}C. The

effect of H_2 initial pressure has been tested at 3.0, 5.0 and 8.0 MPa, while that of catalyst loading with 0.75, 1.5 and 3.0 g of sample.

Gas and liquid samples were analyzed offline. Liquid samples were analyzed by GC (Agilent 7890A, FID, DB-Wax 30 m × 0.53 mm × 1.0 μm). Acetonitrile was used as a solvent for the GC analysis. The liquid products detected were: 2-propenol, 1,2-propanediol (propylene glycol), 1,3-propanediol, ethylene glycol, hydroxyacetone (acetol), 1-propanol, 2-propanol, ethanol and methanol. Gas samples were analyzed in an Agilent GC (7890A, Molecular Sieve and Porapak Q) equipped with thermal conductivity detector (TCD). The only gas-phase product detected under the typical experimental conditions was propylene. The mass balance of all experiments was 90 ± 5%.

Conversion and selectivity values were calculated using the equations described below:

$$Glycerol\ Conversion\ (\%) = \frac{moles\ of\ Glycerol\ In - moles\ of\ Glycerol\ Out * 100}{(moles\ of\ Glycerol\ In)}$$

$$Selectivity\ to\ Product\ i = \frac{Carbon\ moles\ of\ Product\ i * 100}{Total\ Carbon\ moles\ of\ Gas\ and\ Liquid\ Products}$$

2. Results and discussion

Catalyst Characterization

Table 2. Physicochemical catalyst characterization

Catalyst	BET surface area (m^2/g)		Pore Volume (cm^3/g)		TPD-NH_3 (μmol NH_3/m^2 BET)	CO/CO_2 Ratio**
	Fresh	Reduced	Fresh	Reduced	Reduced	Reduced
Activated Carbon (AC)	600	-	0.39 (0.157) *		0.010	-
Carbon Black (BC)	250	-	1.2 (0.0293) *		0.012	-
Mo/BC_A	127	110	0.49	0.44	0.541	13.9
Fe/BC_A	244	239	0.72	1.03	0.034	-
Fe-Mo/BC_A	128	109	0.59	0.60	0.294	16.9
Fe-Mo/AC_A	244	282	0.21 (0.034)*	0.23 (0.063)*	0.233	22.8
Fe-Mo/BC_B	110	105	0.62	0.52	0.315	16.1
Fe-Mo/AC_B	218	277	0.18 (0.044)*	0.23 (0.061)*	0.331	16.4

*Micropore Volume (cm^3/g), ** Results of TPD-He Analysis

Nitrogen Adsorption

The BET Surface areas of all samples, including the catalyst supports', are demonstrated in Table 2. BET areas of all catalysts are significantly lower than those of the supports, as metals fill or block parts of the catalytic pores, thus reducing the surface area. As expected, the BET surface of Fe/BC_A catalyst is close to that of the support due to the low Fe loading. Calcination atmosphere has no significant impact on the surface area of the catalyst. Upon reduction, BET areas of the catalysts

supported on carbon black are further reduced. This decrease is not considered important and suggests that the applied pre-treatment conditions do not affect the surface area[29]. On the other hand, BET surface of the catalysts supported on activated carbon is increased upon reduction, as previously reported[30], because during treatment molybdenum oxide crystals contract and fracture, providing higher surface area. This difference between the samples supported on different carbons is probably due to the porosity of each support. The micropore volume measured for both of the supports validates the presence of microporosity in activated carbon ($0.157 cm^3/g$), in comparison with black carbon ($0.0293 cm^3/g$). After reduction, the microporosity of Fe-Mo/AC catalysts is further increased compared to calcined samples (Table 2); therefore explaining the observed increase in the BET surface area.

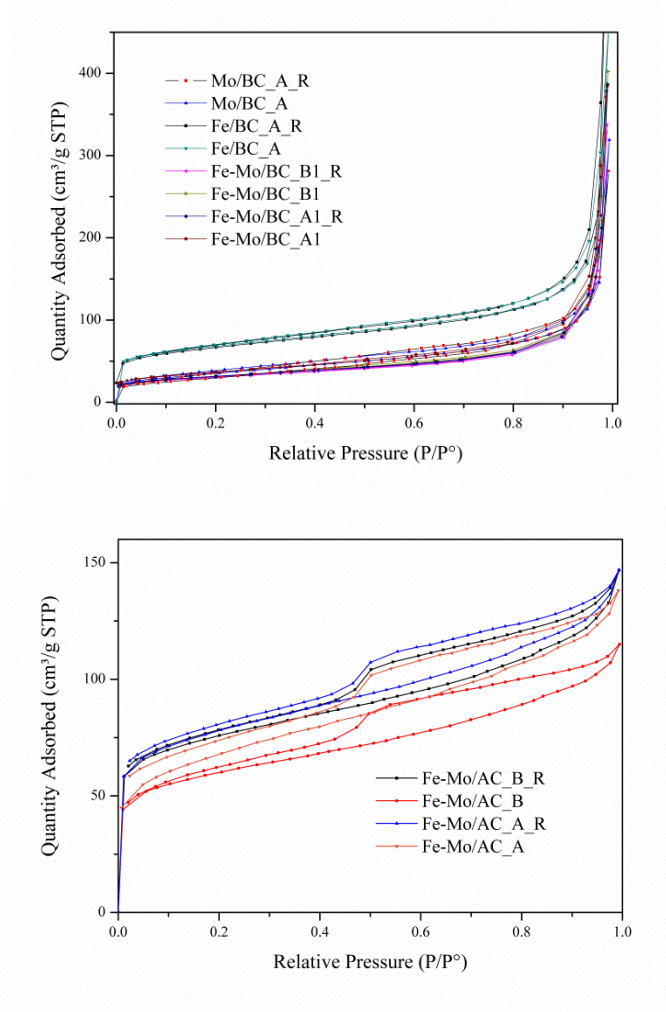

Fig. 1 Adsorption Isotherms a) Catalysts Supported on BC, b) Catalysts Supported on AC

The physisorption isotherms prior to and post reduction treatment are illustrated in Fig. 1, where the letter R stands for reduced samples. Physisorption isotherms of catalysts, supported on carbon black, have gradual curvature that can be associated with macroporous materials. The absence of hysteresis leads to the conclusion that catalysts contain blind cylindrical, wedge-shaped or cone-shaped pores. The isotherms of activated carbon catalysts are typical of microporous materials. Their

hysteresis loop is due to capillary condensation in the catalyst mesopores and this specific type corresponds to narrow spit-like pores[31,32].

X-ray Diffraction (XRD)

The X-ray diffractograms of all fresh samples after calcination are presented in Fig. 2. All catalysts show diffraction peaks that are characteristic of hexagonal MoO_3. There are no peaks attributed to iron oxides, indicating that the oxide is highly dispersed. The broad diffraction peaks of Fe/BC_A catalyst, at 2θ angle of 25 and 44°, are characteristic of black carbon[33] and of the sample holder used for the XRD analysis, respectively. The XRD profiles of the Fe-Mo/AC catalysts differ from the above-mentioned patterns, as the presence of SiO_2 is evident. This is not considered unusual, as Si is one of the main impurities of activated carbons. Presence of $(NH_4)_4Mo_8O_{26}$ in Fe-Mo/BC_A and Fe-Mo/BC_B samples, is probably due to the excess of NH_4OH solution used for co-precipitation in catalyst synthesis procedure and the relatively low calcination temperature (*i.e.* 200^0C). Nonetheless, $(NH_4)_4Mo_8O_{26}$ species were not detected in the reduced samples due to their decomposition and further reduction.

All reduced samples show solely peaks characteristic of MoO_2 (Fig. 3). According to the TPR profiles (Fig. S1), the formation of this molybdenum sub-oxide was expected, as the samples were pre-reduced at 500ºC; this temperature is slightly lower than the T_{max}~520ºC of the first H_2 consumption peak. Compared to literature studies on the reduction patterns of unsupported MoO_3[34], the MoO_3 reduction step ($MoO_3 \rightarrow MoO_2$) appears at lower temperatures in supported Mo and Fe-Mo/C catalysts. However, a closer look at the angle $2\theta=25.87^o$ (Fig. 3b) reveals a shift of the

MoO_2 peak upon Fe addition, which was correspondingly observed for the rest of the peaks attributed to this phase, evidencing an interaction between molybdenum and iron oxides. Despite the fact that only assumptions can be made based on present characterization data, we suggest that the formation of a solid solution is possible, where Mo^{4+} ions of MoO_2-based phase are substituted for Fe ions. [35]

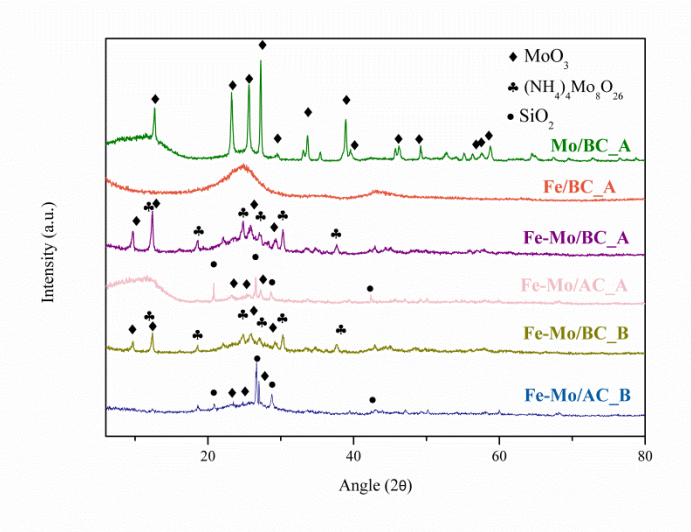

Fig. 2 XRD Diffractograms of Fresh Catalysts

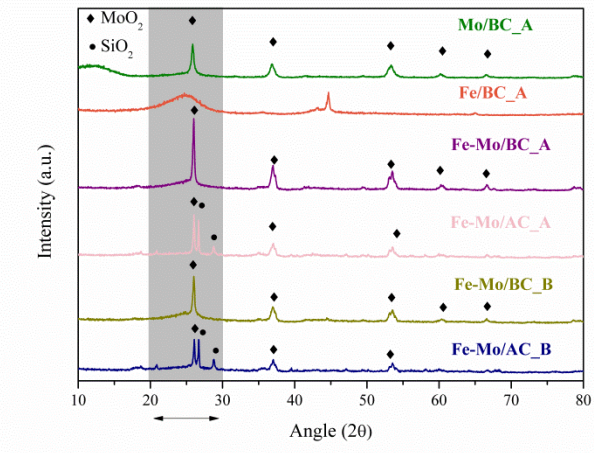

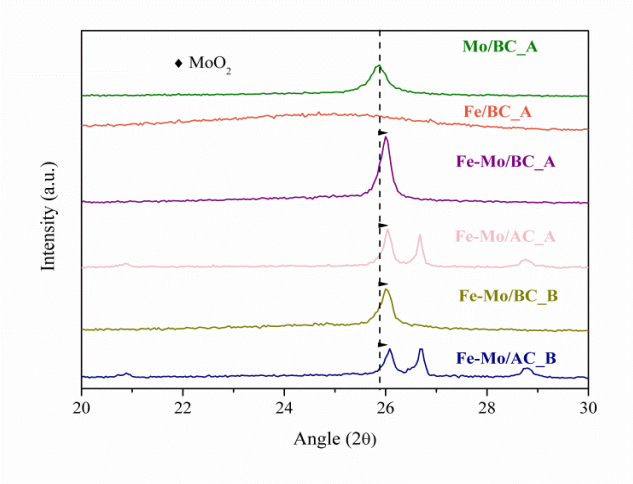

Fig.3 a) XRD Diffractograms of Reduced Catalysts and b) Angle 2θ, 20-30° region shift of the MoO_2 peak

Increased CO/CO_2 ratio, suggesting that more phenolic/quinone groups are present on the surface, compared to carboxylic groups, is related to lower acidity (Table 2). These groups (e.g. phenolic, quinone) have weakly acidic, neutral or even basic character that could affect catalyst activity[36]. Treatment under air flow seems to selectively remove oxygen groups. (Figs S4, S5)

According to TPD-NH_3 data (Fig. S2), high catalyst acidity can be primarily attributed to Mo phases on the surface. The noticeably increased width of MoO_2 XRD peaks in Mo/BC_A catalyst (Fig. 3) indicates high dispersion of MoO_2 that enhances sample acidity, compared to Fe-Mo catalysts. The modification of molybdenum with iron results in surface acidity reduction.

Catalytic Results

The catalytic results of all samples evaluated in glycerol hydro-deoxygenation reaction, at 300°C, are presented on Table 3. Propylene was the only product in the gas phase, while 2-propenol, 1-propanol and propylene glycol were primarily detected in the liquid phase. Other liquid products formed were methanol, 2-propanol, acetol, ethylene glycol, ethanol and 1,3-propanediol.

Carbon supports were also tested as catalysts in the same reaction, nevertheless, in these experiments, glycerol was slightly converted (*i.e.* 0.7 and 6.5%) and only liquid products were formed. In order to examine the role of each metal oxide, (*i.e.* iron and molybdenum), the performance of these samples has also been evaluated. In experiments with Fe/BC_A catalyst, glycerol was also slightly converted to some extent (3.3%), yet only to liquid products. The use of carbon supports and Fe/BC_A as catalysts for the hydro-deoxygenation of glycerol results in the production of liquid products, primarily 2-propenol or propylene glycol (Table 3). Nonetheless, no propene was formed.

The conversion of glycerol over Mo/BC_A was the highest among all catalysts (68.2%), indicating that molybdena species (*i.e.* MoO_2 on the reduced catalysts) drive glycerol hydrodeoxygenation[37]. The higher activity of this catalyst can be attributed to the increased acidity (Table 2), as acidity is considered a key factor, promoting hydro-deoxygenation reactions of glycerol[38-40]. Of great importance is the fact that over Mo/BC_A catalyst, selectivity to gas-phase products (propylene) is mostly favored, compared to selectivity to liquid products; *ca*70% and 30%, respectively. Glycerol conversion over Fe-Mo catalysts is lower compared to the molybdenum catalyst, ranging from 48.9 to 56.0%; lower acidity of Fe-Mo catalysts might be the reason for this. Closer

look at the results of the various Fe-Mo catalysts shows that the type of support (activated vs black carbon) and the calcination atmosphere (N_2 vs air) only marginally affect conversion. Selectivity to gas phase products (propylene) does not seem to be affected by the presence of Fe, as for all Fe-Mo catalysts it remains high and comparable to that of Mo/BC_A. Minor differences are observed for catalysts supported on activated carbon (*i.e.* Fe-Mo/AC_A and Fe-Mo/AC_B), exhibiting slightly lower selectivity (*i.e.* 67.9 and 64.8% respectively) compared to the catalysts supported on black carbon (selectivity to propylene *ca.*71.5%). Different porous characteristics of the catalysts (Table 2) and more specifically, the presence of microporosity in the activated carbon-based catalysts may induce shape selectivity in glycerol transformation, due to the existence of longer diffusion pathways that affect reaction (consumption and formation) rates. Shape selectivity and diffusivity effects on reactant and product rates have been previously reported for carbon materials with microporosity[41,42]. The fact that, under the specific experimental conditions, it appears plausible that propylene readily desorbs from the catalytic active sites and then dissolves in the gas phase[43], due to its low solubility in polar solvents, is of major importance. The latter explains the absence of propane formation via hydrogenation of propylene.

Glycerol deoxygenation is not complete, leading to the formation of partially deoxygenated products, mostly detected in the liquid phase. 2-propenol and propylene glycol are the main products in the liquid phase over molybdena-containing catalysts, although selectivity to these products was significantly lower (Table 3).

As mentioned above, the presence of molybdena sub-oxides on the catalyst surface is essential for the deoxygenation. The reduction procedure and the presence of H_2

atmosphere are key factors for the formation of this active molybdenum phase, along with oxygen vacancies[44], resulting in the production of metallic/acidic bi-functional catalysts[45-47].

Table 3 Catalytic Performance of all Samples in Glycerol HDO reaction (Reaction time: 2.0 h, H_2 pressure: 8.0 MPa, Temperature: 300°C, Catalyst Weight: 1.5g)

Sample	Total Conversion (%)	Selectivity (%)					Yield (%)
		Propene	2-Propenol	1-Propanol	Propylene Glycol	Others*	Propene
Activated Carbon	0.7	0.0	3.1	0.0	53.3	43.6	0.0
Carbon Black	6.5	0.0	11.1	0.0	0.0	88.9	0.0
Fe/BC_A	3.3	0.0	47.7	0.0	0.0	52.3	0.0
Mo/BC_A	68.2	69.9	4.4	7.1	5.4	13.3	47.6
Fe-Mo/BC_A	48.9	71.7	8.0	1.2	7.9	11.2	35.0
Fe-Mo/AC_A	56.0	67.9	10.8	2.7	8.3	10.3	38.0
Fe-Mo/BC_B	51.7	71.5	6.3	4.1	7.8	10.3	37.0
Fe-Mo/AC_B	53.7	64.8	7.5	7.1	8.4	12.2	34.8

*Others refer to Methanol, 2-Propanol, Ethanol, Ethylene glycol, Hydroxyacetone and 1,3PD

Effect of Reaction Parameters

The encouraging above-mentioned results regarding glycerol conversion and selectivity to propene, led to subsequent investigation of the effects of various parameters on glycerol hydro-deoxygenation reaction. The effects of operating conditions (i.e. reaction time, reaction temperature, catalyst loading and H_2 pressure) have been examined and the results are presented below.

Activity and Product Distribution with Time

Experiments to determine the effect of reaction time were performed using the Fe-Mo/BC_A catalyst for 0.5h up to 6h of reaction time. Fig. 4 illustrates the overall glycerol conversion versus reaction time. In general, the overall glycerol conversion gradually increases with time, reaching 88.8% after 6 hours. It should be underlined that at zero time point glycerol has already been partially converted (4.2 %) during the time needed for the temperature to reach the set point. Nevertheless, this value is considered significantly low.

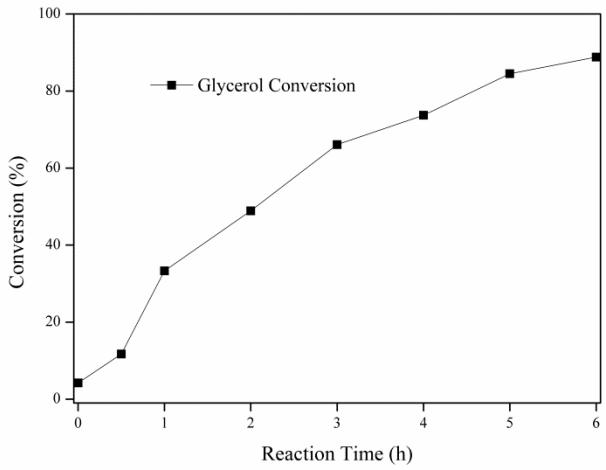

Fig. 4 Reaction Time Effect on Glycerol Conversion over Fe-Mo/BC_A Catalyst (H_2 pressure: 8.0 MPa, Temperature: 300°C)

Fig. 5 illustrates selectivity versus glycerol conversion for the various liquid and gas products formed. The distribution of the reaction products is quite interesting and points out the fact that propene is the main product formed, with 76.1 % selectivity after a six-hour reaction. It must be highlighted that selectivity to propene increases with reaction time (and with glycerol conversion), while a corresponding reduction in 2-propenol selectivity is observed, stressing that 2-propenol is the major intermediate product in propene formation. Experiments, using 2-propenol as feedstock, have been conducted in order to further investigate this hypothesis. Fe-Mo/BC_A catalyst has been employed for this purpose at typical reaction conditions, using 2% wt aqueous 2-propenol initial solution. 2-propenol conversion was significantly high (86.4%), while propene was selectively formed (89.2%); 1- and 2-propanols were also detected, yet, in considerably low concentrations. The high reactivity of 2-propenol, along with the selective formation of propene, stresses that this compound actually is an intermediate product of glycerol hydro- deoxygenation to propene. Glycerol dehydration can lead to the formation of acrolein[48,49], which can be hydrogenated to produce 2-propenol. Despite the fact that acrolein was not detected in the product mixture, it can be inferred that 2-propenol is formed after acrolein hydrogenation. We suggest that 2-propenol is subsequently hydro-deoxygenated to propene (loss of oxygen while preserving the C=C double bond).

Apart from 2-propenol, at low conversion levels, propylene glycol and acetol are the main liquid products formed from glycerol, in 28 and 10% selectivities, respectively, suggesting that a parallel pathway of hydro-deoxygenation is possible via acetol formation and

subsequent hydrogenation to propylene glycol and propanols. However, as glycerol conversion increases, selectivity to these products decreases because propylene glycol converts to 1- and 2-propanols. Selectivity to the rest of the liquid products remains almost constant with glycerol conversion, without showing any considerable change.

The effect of the reaction time on product distribution provides strong evidence regarding propene formation intermediate and reaction pathways. The proposed mechanism follows bi-functional dehydration/hydrogenation pathways. It has been reported that Bronsted acidity directs reaction towards acrolein-propene formation while Lewis acidity towards acetol production[59]. Taking into account the experimental results of this study, as well as relative reports[30,43,51,52], it could be proposed that molybdenum oxide, at reduced state, and surface hydroxyls formed due to water presence and reduction procedure[30,53,54], acting as Brønsted acids, provide the active sites for the reaction to occur. It is of great importance that selectivity to propene increases with glycerol conversion while the overall yield to propene reaches the value of 67.6 %, at 6h of reaction time.

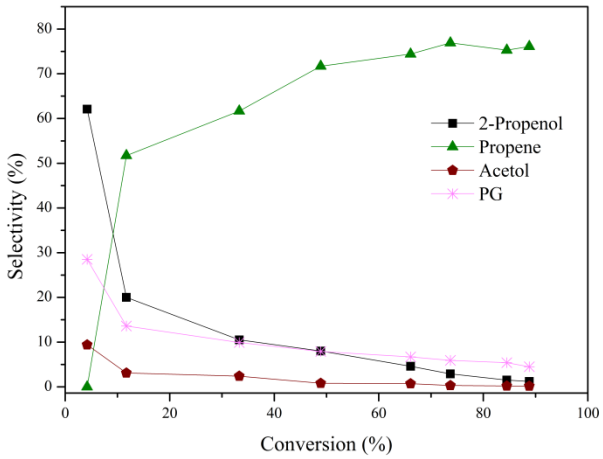

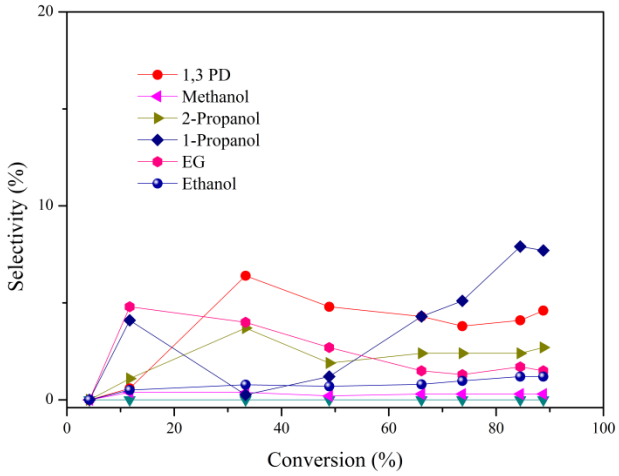

Fig. 5 Reaction Time Effect on Selectivity over Fe-Mo/BC_A Catalyst (H_2 pressure: 8.0 MPa, Temperature: 300°C)

Temperature

In order to determine the effect of temperature on the catalytic results, experiments were performed at 260, 280 and 300°C, using the Fe-Mo/BC_A catalyst. Overall glycerol conversion clearly increases with temperature.

Fig. 6 shows product distribution with temperature, where selectivity to propene noticeably increases. At low temperatures, glycerol dehydration to acetol and subsequent formation of propylene glycol and propanols is favored. Additionally, propylene glycol can be converted to 1- and 2- propanols, explaining the relatively high selectivity of the latter, at 280°C. It has been reported that above 200°C, propylene glycol reacts further to produce mono-alcohols[55]. Selectivity to 2-propenol presents an increase at higher temperature, while no significant change is observed for the rest of the products. As 2-propenol is considered an intermediate product for propene production, its increased

formation at 300°C shows the potential of higher selectivity to propene that could be achieved at the highest temperature used, after 2h of reaction.

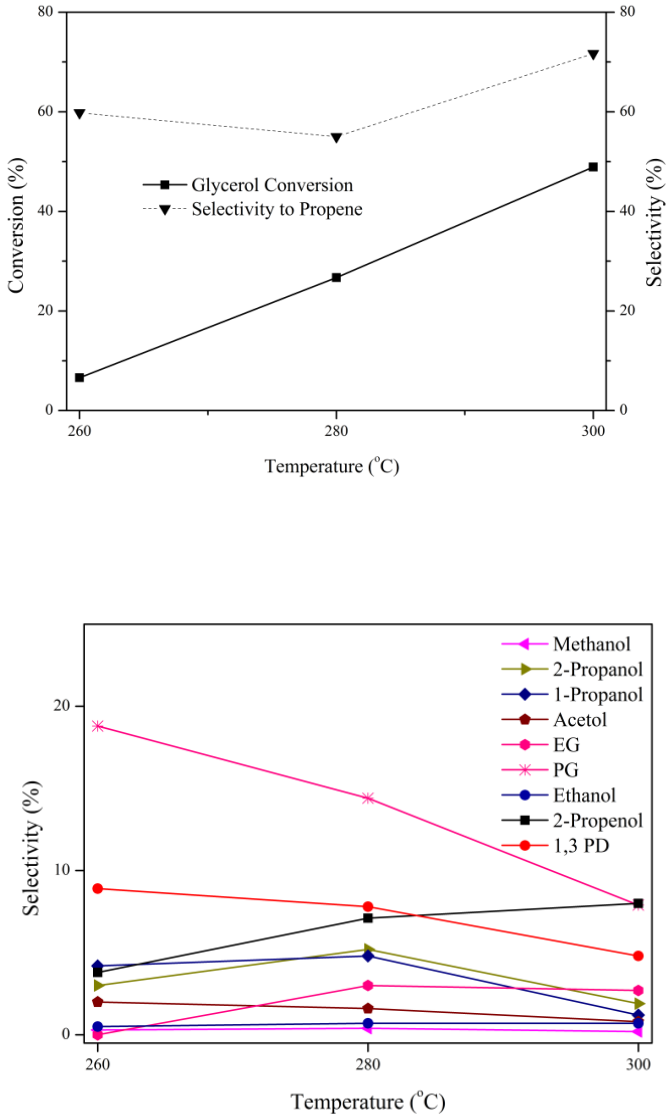

Fig. 6a) Temperature Effect on Glycerol Conversion and Gaseous Product Selectivity, b) on Liquid Product Selectivity, over Fe-Mo/BC_A Catalyst (Reaction time: 2.0 h, H_2 pressure: 8.0 MPa)

Catalyst Loading

Experiments were performed with different catalyst loadings (*i.e.* 0.75g, 1.5g and 3.0g) using the Fe-Mo/BC_A catalyst. As expected, glycerol conversion increases with the catalyst amount (Fig. 7). The results specify that incremental addition of catalyst, providing more active sites, enhances glycerol conversion[56]. However, it is observed that by doubling the catalyst weight, from 1.5 to 3g, the conversion does not increase proportionally, indicating possible mass transfer effects at high catalyst concentrations. Variations of the catalyst weight also affect the product distribution. Increase of the catalyst amount, up to 1.5g, leads to higher selectivity to propene, mostly because of higher conversion. In contrast, further increase of conversion, from 50 to 65%, is not followed by enhanced propene selectivity, probably due to sequential propene hydration to propanols[57]. Indeed, selectivity to 2- and 1-propanol increases considerably.

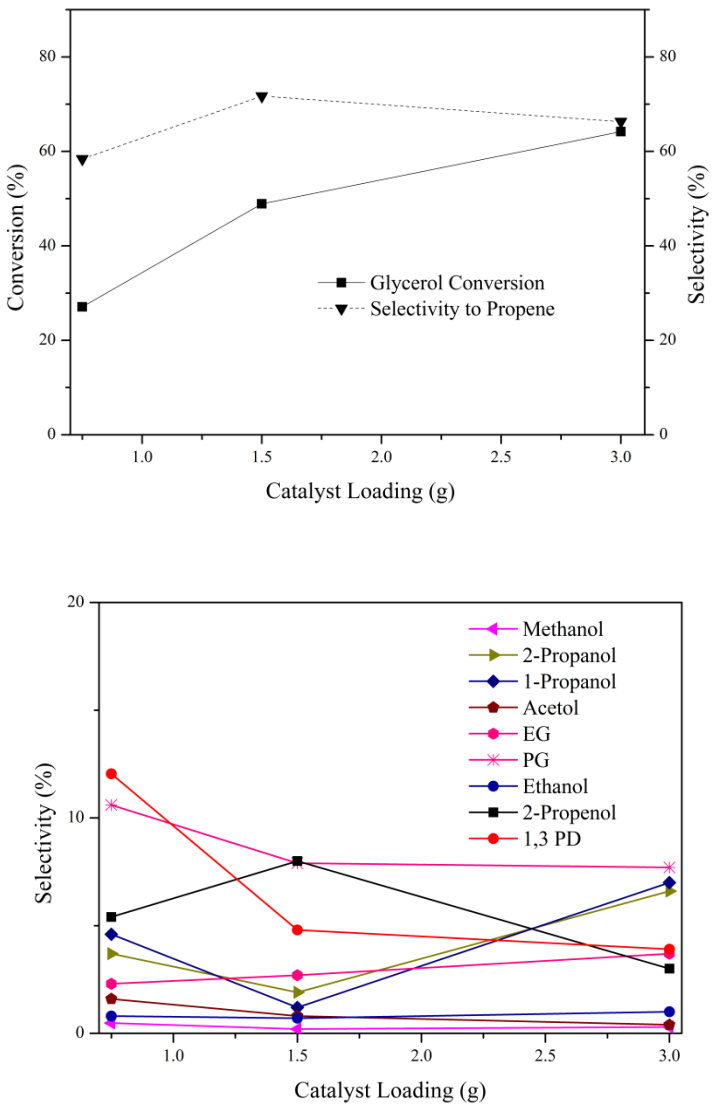

Fig. 8 a) Effect of Catalyst Loading on Glycerol Conversion and Gaseous Product Selectivity, b) on Liquid Product Selectivity over Fe-Mo/BC_A Catalyst (Reaction time: 2.0 h, H_2 pressure: 8.0 MPa, Temperature: 300ºC)

H_2 Pressure

Experiments were performed by differentiating the H_2 initial pressure (*i.e.* 3.0, 5.0, and 8.0 MPa), over the Fe-Mo/BC_A catalyst. Increased H_2 pressure has a positive effect on glycerol conversion (Fig. 8). High pressure favors H_2 solubility in water, thus, increasing its concentration in the liquid phase[16]. At lower pressure, selectivity to alcohols is increased while after 5.0 MPa, selectivity to most of the products of the liquid phase decreases. Low selectivity to propene, especially at 3MPa cannot be ascribed solely to low conversion levels but primarily to the low hydrogenation extent due to limited H_2 availability. The critical role of H_2 availability for propene selectivity explains the relatively lower values obtained in the present study, compared to those mentioned by Fadigas et al.[28].

In this study, H_2/Glycerol molar ratio is ~53:1(~88% conversion and ~76% selectivity to propene), while the optimum ratio used by Fadigas et al.[28] is 120:1 (100% conversion and ~90% selectivity to propene; the gas phase products observed were propane, ethane and methane, apart from propene. Moreover, the optimum H_2/Glycerol molar ratio used by Cao et al. is 100:1 (100% conversion and 85% selectivity to propene), while the main by-product formed was propane [27]. Nevertheless, according to the present catalytic results, under the specific reaction conditions, propene is the only gas-phase product formed (100% selectivity in the gas phase).

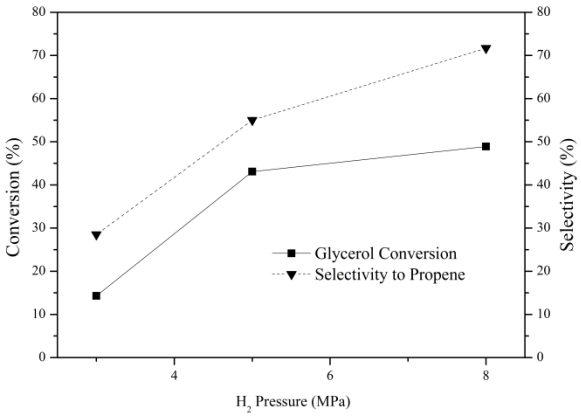

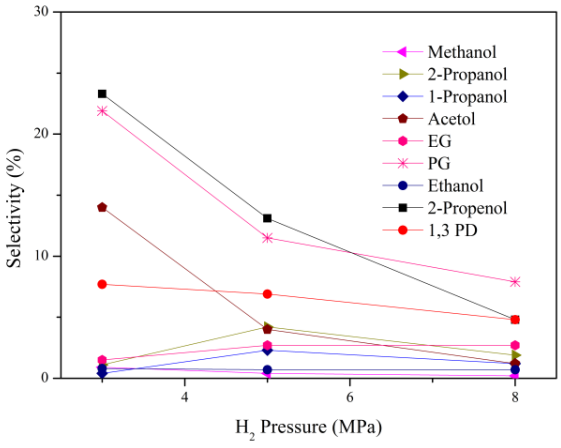

Fig.4 a) H_2 Pressure Effect on Glycerol Conversion and Gaseous Product Selectivity, b) on Liquid Product Selectivity, over Fe-Mo/BC_A Catalyst (Reaction time: 2.0 h, Temperature: 300ºC)

Catalyst Re-use Experiments

Fe-Mo/BC_A catalyst has been re-used under the standard reaction conditions in order for its stability to be evaluated. Four consecutive experiments have been conducted at the standard reaction conditions (i.e. H_2 pressure: 8.0 MPa, Temperature: 300ºC) for 4h; prior to each test, the

catalyst was reduced, following the typical procedure. According to the experimental data, glycerol conversion is decreased by 10% after the fourth recycle experiment. It must be highlighted that deactivation affects only catalyst activity and not selectivity to propene, as the latter follows glycerol conversion decrease (Fig.5a). The above results highlight the structural integrity of the Fe-Mo/BC_A catalyst.

4. Conclusions

Propene can be effectively produced via one-step HDO reaction of glycerol derived from biomass, in the liquid phase, over Fe-Mo/C catalysts. After 6h of reaction time, glycerol can be converted up to 88.8% with 76.1 % overall selectivity to propene (100% in gas phase). Fe-Mo catalysts were synthesized, characterized and their activity has been evaluated. Characterization results indicate that molybdenum sub-oxide (*i.e.* MoO_2) is the active phase of these reactions. Under reaction conditions of this research (Temperature and Pressure: 300ºC and 8.0MPa, respectively) Fe-Mo catalysts are active to the selective conversion of glycerol to propylene. Increased temperature and H_2 pressure (*i.e.* H_2/glycerol ratio) favor glycerol conversion towards propene, while suppress formation of acetol, propanols and propane-diols. Higher catalyst loading also directs reaction to the formation of the desired product, in the gas phase. The evolution of reaction products as a function of reaction time suggests that propene is mainly formed via the acrolein-2-propenol route while the contribution of the acetol-propylene glycol-2-propanol route is rather limited. Stability tests reveal that selectivity to propene is not affected by the moderate activity loss (10%) observed after the fourth re-use test, as it clearly follows the reduction of glycerol conversion.

Acknowledgements

This research has been co-financed by the European Union (European Social Fund – ESF) and Greek national funds through the Operational Program "Education and Lifelong Learning" of the National Strategic Reference Framework (NSRF) - Research Funding Program: THALIS. Investing in knowledge society through the European Social Fund.

References

1 A. M. Ruppert, K. Weinberg and R. Palkovits, *Angew. Chem. Int. Ed.*, 2012, **51**, 2564–2601.

2 P. Basu, *Biomass Gasification and Pyrolysis*, Elsevier, USA, 2010, pp. 325–326.

3 G. W. Huber, S. Iborra and A. Corma, *Chem. Rev.*, 2006, **106**, 4044–4098.

4 P. N. R. Vennestrøm, C. M. Osmundsen, C. H. Christensen and E. Taarning, *Angew. Chem. Int. Ed.*, 2011, **50**, 10502–10509.

5 T. Werpy and G. Petersen, *Top Value Added Chemicals from Biomass*, N.R.E.L., U.S. Department of Energy, USA, 2004, available online at http:/www.osti.gov/bridge.

6 L. R. Morrison, in *Kirk-Othmer Encyclopedia of Chemical Technology*, John Wiley and Son Inc., 2000, DOI: 10.1002/0471238961.0712250313151818.a01.

7 Z. Wang, J. Zhuge, H. Fang and B. A. Prior, *Biotechnol. Adv.*, 2001, **19**, 201–223.

8 F. N. Arroyo-López, R. Pérez-Torrado, A. Querol and E. Barrio, *Food Microbiol.*, 2010, **27**, 628–637.

9 T. Modig, K. Granath, L. Adler and G. Lidén, *Appl. Microbiol. Biotechnol.*, 2007, **75**, 289–296.

10 H. Zhao, C. H. Zhou, L. M. Wu, J. Y. Lou, N. Li, H. M. Yang, D. S. Tong and W. H. Yu, *Appl. Clay Sci.*, 2013, **74**, 154–162.

11 F. Bauer and C. Hulteberg, *Biofuels, Bioprod. Bioref.*, 2013, **7**, 43–51.

12 E. S. Vasiliadou and A. A. Lemonidou, *Appl. Catal. A Gen.*, 2011, **396**, 177–185.

13 D. Lahr and B. Shanks, *J. Catal.*, 2005, **232**, 386–394.

14 E. S. Vasiliadou, E. Heracleous, I. A. Vasalos and A. A. Lemonidou, *Appl. Catal. B Environ.*, 2009, **92**, 90–99.

15 E. S. Vasiliadou, T. M. Eggenhuisen, P. Munnik, P. E. de Jongh, K. P. de Jong and A. A. Lemonidou, *Appl. Catal. B Environ.*, 2014, **145**, 108–119.

16 E. S. Vasiliadou and A. A. Lemonidou, *Chem. Eng. J.*, 2013, **231**, 103–112.

17 A. K. Kinage, P. P. Upare, P. Kasinathan, Y. K. Hwang and J. S. Chang, *Catal. Commun.*, 2010, **11**, 620–623.

18 S. Chai, H. Wang, Y. Liang and B. Xu, *J. Catal.*, 2007, **250**, 342–349.

19 E. Tsukuda, S. Sato, R. Takahashi and T. Sodesawa, *Catal. Commun.*, 2007, **8**, 1349–1353.

20 H. Serafim, I. M. Fonseca, A. M. Ramos, J. Vital, and J. E. Castanheiro, *Chem. Eng. J.*, 2011, **178**, 291–296.

21 Y. Amada, S. Koso, Y. Nakagawa and K. Tomishige, *ChemSusChem*, 2010, **3**, 728–736.

22 K. Murata, I. Takahara and M. Inaba, *React. Kinet. Catal. Lett.*, 2008, **93**, 59–66.

23 J. van Haveren, E. L. Scott and J. Sanders, *Biofuels, Bioprod. Bioref.*, 2008, **2**, 41–57.

24 B. A. Rodriguez, C. C. Stowers, V. Pham and B. M. Cox, *Green Chem.*, 2014, **16**, 1066-1076.

25 G. M. Wells, *Handbook of Petrochemicals and Processes*, Gower Publishing Company Limited, Great Britain, 1991.

26 *US Pat.*, 0 224 470, 2011.

27 L. Yu, J. Yuan, Q. Zhang, Y.-M. Liu, H.-Y. He, K.-N. Fan and Y. Cao, *ChemSusChem*, 2014, **7**, 743-747.

28 *WO Pat.*, 155 674 2009.

29 O. Bayraktar, Ph.D. Thesis, West Virginia University, 2001.

30 T. Matsuda, Y. Hirata, H. Sakagami and N. Takahashi, *Chem. Lett.*, 1997.

31 G. Leofanti, M. Padovan, G. Tozzola and B. Venturelli, *Catal. Today*, 1998, **41**, 207–219.

32 K. S. W. Sing, D. H. Everett, R. H. W. Haul, L. Moscou, R. A. Pierotti, J. Rouquerol and T. Siemieniewska, *Pure & Appl. Chem.*, 1985, **57**, 603–619.

33 J. Wang, G. Yin, Y. Shao, S. Zhang, Z. Wang and Y. Gao, *J. Power Sources*, 2007, **171**, 331–339.

34 K. V. R. Chary, K. R. Reddy, G. Kishan, J. W. Niemantsverdriet and G. Mestl, *J. Catal.*, 2004, **226**, 283–291.

35 Y. Huang, L. Cong, J. Yu, P. Eloy and P. Ruiz, *J. Mol. Catal. A Chem.*, 2009, **302**, 48–53.

36 J. Vissers, S. Bouwens, V. de Beer and R. Prins, *Carbon* , 1987, **25**, 485–493.

37 H. Ren, W. Yu, M. Salciccioli, Y. Chen, Y. Huang, K. Xiong, D. G. Vlachos, and J. G. Chen, *ChemSusChem*, 2013, **6**, 798–801.

38 C.H. Zhou, J. N. Beltramini, Y.X. Fan and G. Q. Lu, *Chem. Soc. Rev.*, 2008, **37**, 527–549.

39 Y. Zheng, X. Chen and Y. Shen, *Chem. Rev.*, 2008, **108**, 5253–5277.

40 B. Katryniok, S. Paul, M. Capron and F. Dumeignil, *ChemSusChem*, 2009, **2**, 719–730.

41 S. M. Csicsery, *Zeolites*, 1984, **4**, 202-213.

42 P. B. Weisz, *Pure Appl. Chem.*, 1980, **52**, 2091–2103.

43 D. R. Moberg, T. J. Thibodeau, F. G. Amar and B. G. Frederick, *J. Phys. Chem. C,* 2010, **114**, 13782–13795.

44 T. Prasomsri, T. Nimmanwudipong and Y. Román-Leshkov, *Energy Environ. Sci.*, 2013, **6**, 1732.

45 F. C. Meunier, F. Cavallaro, T. Le Goaziou, A. Goguet and C. Rioche, *Catal. Today*, 2006, **112**, 64–67.

46 A. Katrib, P. Leflaive, L. Hilaire and G. Maire, *Catal. Letters*, 1996, **38**, 95–99.

47 E. Torres-García, G. Rodríguez-Gattorno, J. A. Ascencio, L. O. Aleman-Vazquez, J. L. Cano-Domínguez, A. Martínez-Hernandez and P. Santiago-Jacinto, *J. Phys.*

Chem. B, 2005, **109**, 17518–17525.

48 A. Corma, G. Huber, L. Sauvanaud and P. O'Connor, *J. Catal.*, 2008, **257**, 163–171.

49 L. Shen, H. Yin, A. Wang, X. Lu, C. Zhang, F. Chen, Y. Wang and H. Chen, *J. Ind. Eng. Chem.*, 2014, **20**, 759–766.

50 A. Alhanash, E. F. Kozhevnikova and I. V. Kozhevnikov, *Appl. Catal. A Gen.*, 2010, **378**, 11–18.

51 H. Sakagami, T. Ohno, H. Itoh, Z. Li, N. Takahashi and T. Matsuda, *Appl. Catal. A Gen.*, 2014, **470**, 8–14.

52 C. Hoang-Van, O. Zegaoui, *Appl. Catal. A Gen.*, 1995, **130**, 89–103.

53 H. Al-Kandari, A. M. Mohamed, F. Al-Kharafi, M. I. Zaki and A. Katrib, *Appl. Catal. A Gen.*, 2012, **417-418**, 298–305.

54 H. Belatel, H. Al-Kandari, F. Al-Khorafi, A. Katrib and F. Garin, *Appl. Catal. A Gen.*, 2004, **275**, 141–147.

55 M. A. Dasari, P.P. Kiatsimkul, W. R. Sutterlin and G. J. Suppes, *Appl. Catal. A Gen.*, 2005, **281**, 225–231.

56 N. Dimitratos, A. Villa and L. Prati, *Catal. Letters*, 2009, **133**, 334–340.

57 M. E. Thibault, D. V. DiMondo, M. Jennings, P. V. Abdelnur, M. N. Eberlin and M. Schlaf, *Green Chem.*, 2011, **13**, 357-366.

Table of contents entry

Textual Abstract

A novel one-step process is explored for glycerol conversion to propene, over Molybdena-based catalysts. Via Hydro-deoxygenation reactions, glycerol is converted to 2-propenol, which is subsequently hydrogenated to form propene.

Graphical Abstract